33rd Annual International Conference of the IEEE EMBS
Boston, Massachusetts USA, August 30 - September 3, 2011

Inclusion Mechanical Property Estimation using Tactile Images, Finite Element Method, and Artificial Neural Network

Jong-Ha Lee, *Student Member, IEEE,* Chang-Hee Won, *Member, IEEE*

Abstract— **In this paper, we developed a methodology for estimating three parameters of tissue inclusion: size, depth, and Young's modulus from the tactile data obtained at the tissue surface with the tactile sensation imaging system. The estimation method consists of the forward algorithm using finite element method, and inversion algorithm using artificial neural network. The forward algorithm is designed to comprehensively predict the tactile data based on the mechanical properties of the tissue inclusion. This forward information is used to develop an inversion algorithm that will be used to extract the size, depth, and Young's modulus of a tissue inclusion from the tactile image. The proposed method is then validated with custom made tissue phantoms with matching elasticities of typical human breast tissues. The experimental results showed that the proposed estimation method estimates the size, depth, and Young's modulus of tissue inclusions with root mean squared errors of 1.25 mm, 2.09 mm, and 28.65 kPa, respectively.**

I. INTRODUCTION

It is widely known that tumors and cancerous tissues are stiffer than the surrounding normal tissues [1]. Thus, tissue inclusion stiffness as well as its geometry measurement can help early detection of malignant tumors such as breast cancer. To help physicians to detect tumors more efficiently various methods have been devised to measure the elasticity of the tissues and embedded lumps [2], [3].

Elastography is a non-invasive method in which tissue elasticity is used to detect and classify tumors [4]. If a compression or vibration is applied to the tissue, the embedded tumor deforms less than the surrounding tissue due to its high stiffness characteristics. Under this observation, elastography records the distribution of tissue elasticity using sound waves. While elastography is successfully applied to static organs such as liver, breast, and brain, the calculation of tissue inclusion stiffness is challenging. Also the instrument is relatively expensive and requires a dedicated operator [5], [6].

The medical device named "SureTouch Visual Mapping System" produced by Medical Tactile Inc. uses capacitive pressure sensor array to measure the tissue elasticity [7]. The device is capable of computing and visualizing the pressure pattern of the tissue. However, the resolution of pressure sensor based method is not as good as optical based method. Also this system requires other sensors to detect the applied force. Another type of elasticity determination system using tactile sensor is the "piezoelectric finger (PEF)" [8]. In this work, the micromachined artificial finger, using piezoelectric tactile sensing mechanism, is introduced. PEF has several advantages including low cost, small form factor, and large dynamic range. However, PEF is sensitive to temperature variation, thus requiring somewhat extensive calibration. Furthermore, limited spatial resolution and hysteresis are the disadvantages of PEF system.

To estimate parameters of tissue inclusions through the obtained tactile data, a novel estimation method is needed. In [9], 2-dimensional (2-D) finite element method (FEM) based forward algorithm and Gaussian fitting model-based inversion algorithms are devised. This work was extended in [10] to find a more complete set of tissue inclusions. They showed that the estimation result is more accurate in determining the size of a tissue inclusion than manual palpation. Nevertheless, the results are limited to tissue inclusion at least 100 times stiffer than the surrounding tissues. The FEM based forward algorithm and artificial neural network (ANN) based inversion algorithm is also proposed in [11]. But in their work, the FEM modeling was done in 2-D, however, the tissue phantom is 3-dimensional (3-D). Thus 2-D model is not an accurate representation of the phantom. Furthermore, the small number of 2-D FEM data used to train the inversion algorithm also makes the parameter estimation results less accurate.

In this paper, a novel estimation method to quantify various tissue inclusion parameters such as size, depth, and Young's modulus is presented. The estimation is performed based on the tactile data obtained at the tissue surface using the tactile sensation imaging system (TSIS) [12]. To estimate tissue inclusion parameters, finite element method and artificial neural network algorithms are utilized. FEM is used to generate simulated tactile data over different tissue inclusion parameters (size, depth, and elasticity) in the idealized tissue model. ANN is used to map the simulated tactile data to the tissue inclusion parameters. To verify the proposed method, the realistic tissue phantom experiments are performed.

In the following section, the design concept and imaging principle of TSIS are introduced. Next, the inclusion parameter estimation method is discussed. We use forward modeling (FEM) and invese modeling (neural networks). Then the proposed estimation method is validated using the custom made tissue phantoms. Finally, the conclusions are presented.

This work was supported in part by the Tobacco Formula Fund (Pennsylvania Department of Health) through Temple University Office of the Senior Vice Provost for Research and Graduate Education, and Germinator Fund Program from BioStrateg Partners.

J.-H. Lee is a research assistant in the Department of Electrical and Computer Engineering, Temple University, Philadelphia, PA 19122 USA jong@temple.edu

C.-H. Won is an associate professor in the Department of Electrical and Computer Engineering, Temple University, Philadelphia, PA 19122 USA cwon@temple.edu

II. TACTILE SENSATION IMAGING SYSTEM

In this section, we present the design concept and imaging principle of TSIS.

A. System Overview

Fig. 1 shows the schematic of TSIS. The system incorporates an optical waveguide unit (2.5cm x 2.5cm), a light source unit (LEDs), a high resolution camera unit, and a computer unit. The optical waveguide unit is the main sensing probe of the system. The waveguide is composed of multi-layered polydimethylsiloxane (PDMS), which is a high performance silicone elastomer [13]. Our high resolution CMOS camera has 8.4 μm $\times$ 9.8 μm individual pixel size (Allied Vision Technology, Germany). It has a pixel array of 768 (H) $\times$ 492 (V) with 8 bit depth. The camera is placed below a waveguide. A glass plate is placed between camera and waveguide. The internal light source is a white LED with a diameter of 1.5 mm. There are four LED light sources placed on four sides of the waveguide to provide illumination.

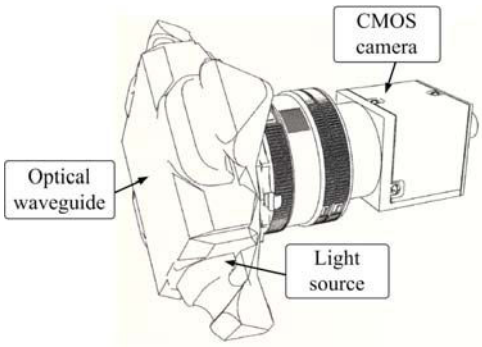

Fig. 1: The schematic of tactile sensation imaging system.

B. Tactile Sensation Imaging Principle

TSIS operates based on the optical phenomenon known as the total internal reflection (TIR) principle of light in the waveguide [14]. To achieve TIR in the waveguide, light is injected into the waveguide under the acceptance angle [12]. Then the light is totally reflected. After trapping the light in the waveguide, if the waveguide is compressed by an external force due to the stiff tissue inclusion, the contact area of the waveguide deforms and causes the light to scatter. The scattered light is then captured by the high resolution camera and saved it as an image. Fig. 2(a) and 2(b) illustrates the conceptual diagram of the sensing principle.

C. Example of Tissue Inclusion Detection

To get a sample tactile data of tissue inclusion, a realistic tissue phantom with 2 mm diameter spherically shaped inclusion is purchased from MammaCare Corp., FL. Using TSIS, the tactile data of a tissue inclusion is obtained. Fig. 3(a) shows the imaging experiment to obtain the tactile data of tissue inclusion using TSIS. Fig. 3(b) shows the initial gray scale tactile data. In Fig. 3(c), a false color scale is used on the original gray scale for the clearer visualization.

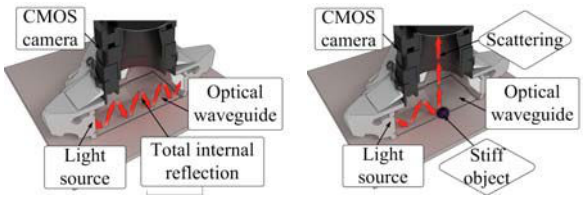

(a) (b)

Fig. 2: The concept of the tactile sensation imaging principle. (a) The light is injected into the waveguide to totally reflect. (b) The light scatters as the waveguide deforms due to the stiff tissue inclusion.

Then the 3-D reconstruction is performed based on the pixel value as the depth information.

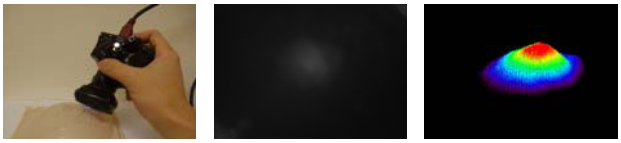

(a) (b) (c)

Fig. 3: The tactile sensation imaging experiment for a breast tissue inclusion. (a) Obtaining tactile data of a tissue inclusion using TSIS, (b) Raw gray scale tactile data, (c) Color visualization with 3-D reconstruction.

III. TISSUE INCLUSION PARAMETER ESTIMATION

In this section, we present a tissue inclusion's parameter estimation method to determine the absolute stiffness and geometric information. We use tactile images obtained from TSIS. The method consists of finite element method (FEM) based forward algorithm, and artificial neural network (ANN) based inversion algorithm.

A. Problem Formulation

To estimate embedded lump mechanical properties, forward and inversion algorithms were developed based on the idealized tissue model. The assumptions used in the model are similar to those used in [9]. The tissue is assumed as a slab of material of constant thickness that is fixed to a flat, incompressible chest wall. The tissue inclusion is assumed to be spherical. Both tissue and inclusion are assumed linear and isotropic. The interaction between TSIS and tissue is assumed to be frictionless.

B. Forward Algorithm

The forward algorithm is designed to investigate the relationship between tissue inclusion parameters and tactile data. In this paper, 3-D FEM is considered for the forward algorithm. The FEM modeling is performed based on the idealized tissue model using ANSYS version 11.0, an engineering simulation software package. The designed FEM model is shown in Fig. 4.

If TSIS compresses against the tissue surface containing a stiff tissue inclusion, the sensing probe of TSIS deforms.

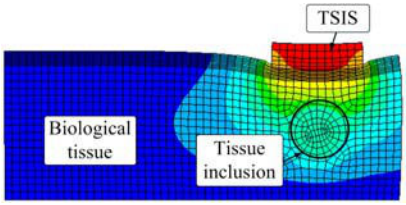

Fig. 4: The FEM model based on the idealized tissue model.

Throughout FEM, the deformed shape of sensing probe is captured in response to different inclusion parameters, size d, depth h, and Young's modulus E. To quantify the amount of sensing probe deformation, the following definitions are used: Maximum deformation, O^1_{FEM}, is defined as the largest vertical displacement of the FEM element of sensing probe from the non-deformed position. Total deformation, O^2_{FEM}, is defined as the vertical displacement summation of FEM elements of sensing probe from the non-deformed position. Deformation area, O^3_{FEM}, is defined as the projected area of the deformed surface.

In the FEM based forward algorithm, (d, h, E) are input variables and maximum deformation, O^1_{FEM}, total deformation, O^2_{FEM}, and deformation area, O^3_{FEM}, of sensing probe are output variables. To investigate the relationship between the input variables (d, h, E) and the output variables (O^1_{FEM}, O^2_{FEM}, O^3_{FEM}), 134 input variables (d, h, E) are randomly generated with the minimum and maximum constraints of d as [2 mm; 13 mm], h as [4 mm; 12 mm], and E as [40 kPa; 120 kPa] [1]. Then 134 output variables (O^1_{FEM}, O^2_{FEM}, O^3_{FEM}) corresponding to 134 input variables (d, h, E) are investigated using FEM.

C. Mapping Tactile Data

It is necessary to relate FEM tactile data (O^1_{FEM}, O^2_{FEM}, O^3_{FEM}) and TSIS tactile data (O^1_{TSIS}, O^2_{TSIS}, O^3_{TSIS}). To map two different tactile data, the calibration tissue phantom with 9 embedded stiff inclusions has been manufactured by CIRS, Inc., VA. This calibration tissue phantom was made of a silicone composite having Young's modulus of approximately 5 kPa. The inclusion was made using another silicone composite with the stiffness higher than the surrounding tissue phantom. We custom designed this calibration tissue phantom with varying parameters (d, h, E) as shown in Table I.

TABLE I: The size, d, depth, h, and Young's modulus, E, of 9 inclusions in the calibration tissue phantom.

Number	Size (d)	Depth (h)	Modulus (E)
1	2 mm	5 mm	120 kPa
2	8 mm	5 mm	120 kPa
3	13 mm	5 mm	120 kPa
4	7 mm	4 mm	100 kPa
5	7 mm	8 mm	100 kPa
6	7 mm	12 mm	100 kPa
7	10 mm	5 mm	40 kPa
8	10 mm	5 mm	70 kPa
9	10 mm	5 mm	100 kPa

To map TSIS tactile data to FEM tactile data, tactile data of 9 inclusions in tissue phantoms were obtained using TSIS. In order to quantify TSIS tactile data, maximum pixel value, O^1_{TSIS}, total pixel value, O^2_{TSIS}, and deformation area of pixel, O^3_{TSIS}, of TSIS tactile data are computed. The definitions of (O^1_{TSIS}, O^2_{TSIS}, O^3_{TSIS}) are as follows. Maximum pixel value, O^1_{TSIS}, is defined as the pixel value in the centroid of the tactile data. Total pixel value, O^2_{TSIS}, is defined as the summation of pixel values in the tactile data. Deformation area of pixel, O^3_{TSIS}, is defined as the number of pixel greater than the specific threshold value k in the tactile data. We assume that there is no noise in the tactile data.

To find the relationship between TSIS tactile data to FEM tactile data, the graphs of (O^1_{FEM} : O^1_{TSIS}), (O^2_{FEM} : O^2_{TSIS}), and (O^3_{FEM} : O^3_{TSIS}) were generated. Then using the linear regression method, the relationship between TSIS tactile data to FEM tactile data is found. Figs. 5(a) to 5(c) represent linear regression results. Since the tactile data is normalized, three data in each graph exists in the same position (1,1). Using these three relationships, the newly obtained TSIS tactile data (O^1_{TSIS}, O^2_{TSIS}, O^3_{TSIS}) can be transformed into the FEM tactile data (O^1_{FEM}, O^2_{FEM}, O^3_{FEM}). In this way, we relate TSIS tactile data with FEM tactile data.

D. Inversion Algorithm

The goal of an inversion algorithm is to estimate (d, h, E) through obtained TSIS tactile data (O^1_{TSIS}, O^2_{TSIS}, O^3_{TSIS}). We estimate(O^1_{FEM}, O^2_{FEM}, O^3_{FEM}) from (O^1_{TSIS}, O^2_{TSIS}, O^3_{TSIS}) using calibrated data. Then we design an inversion algorithm to estimate (d, h, E) using the determined (O^1_{FEM}, O^2_{FEM}, O^3_{FEM}).

In this paper, the multi-layered artificial neural network (ANN) is considered as an inversion algorithm [15]. To train ANN, 125 input variables (O^1_{FEM}, O^2_{FEM}, O^3_{FEM}) and corresponding output variables (d, h, E) are used. The remaining 9 (d, h, E) variables, which are used for the calibration tissue phantom design, are used for the validation of the proposed estimation method. For the training on ANN algorithm, scaled conjugate gradient algorithm (SCGA) is used due to its simple and robustness characteristics [15].

IV. Experimental Results

To validate the proposed estimation method, tactile data of 9 tissue inclusions in the calibration tissue phantom were obtained using TSIS. TSIS tactile data was then quantified as (O^1_{TSIS}, O^2_{TSIS}, O^3_{TSIS}). Using the quantified data, (O^1_{TSIS}, O^2_{TSIS}, O^3_{TSIS}), we estimated tissue inclusion parameters, ($\hat{d}$, $\hat{h}$, $\hat{E}$). To measure the performance of the proposed estimation method, the cross validation method called leave-one-out-cross-validation (LOOCV) metric was considered [16]. The estimation of each tissue inclusion parameters ($\hat{d}$, $\hat{h}$, $\hat{E}$) were performed 100 times per each inclusion and the results were averaged. The averaged estimation results of each inclusion are shown in Table II.

The final validation was performed using the root mean squared error (RMSE). Let T be the true inclusion parameters (d, h, E) in Table I, and Y be the estimated inclusion

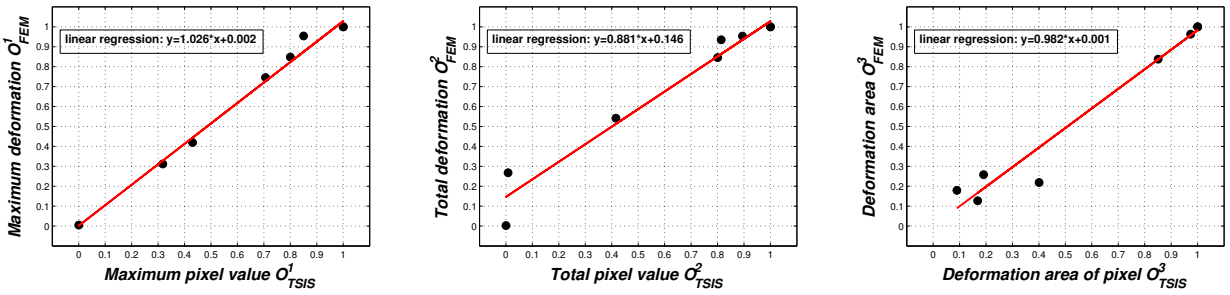

(a) (b) (c)

Fig. 5: The linear regression results between FEM tactile data and TSIS tactile data. The linear regression result between (a) maximum deformation O^1_{FEM} and maximum pixel value O^1_{TSIS}, (b) total deformation O^2_{FEM} and total pixel value O^2_{TSIS}, (c) deformation area O^3_{FEM} and deformation area O^3_{TSIS}.

TABLE II: The estimated average size, $\hat{d}$, depth, $\hat{h}$, and Young's modulus, $\hat{E}$, of 9 inclusions in the calibration tissue phantom.

Number	Est. size ($\hat{d}$)	Est. depth ($\hat{h}$)	Est. modulus ($\hat{E}$)
1	4.11 mm	8.52 mm	74.52 kPa
2	8.11 mm	7.06 mm	83.97 kPa
3	10.73 mm	5.81 mm	79.46 kPa
4	5.77 mm	7.97 mm	78.29 kPa
5	4.91 mm	8.23 mm	78.06 kPa
6	4.94 mm	8.45 mm	77.87 kPa
7	10.11 mm	6.29 mm	84.84 kPa
8	10.74 mm	6.11 mm	76.96 kPa
9	10.57 mm	7.33 mm	82.21 kPa

parameters ($\hat{d}$, $\hat{h}$, $\hat{E}$) in Table II. Then RMSE e_j can be calculated as follows.

$$e_j = \sqrt{\frac{1}{n} \times \sum_{i=1}^{n} (T_{ij} - Y_{ij})^2}, \quad (1)$$

where i is the number of inclusions which is 9 and j is the number of tissue inclusion parameters which is 3 in our case. Table III shows RMSE of all inclusion parameter estimation results.

TABLE III: The root mean squared error (RMSE) of 9 inclusions parameter estimation.

Inclusion parameter	RMSE
Size ($\hat{d}$)	1.25 mm
Depth ($\hat{h}$)	2.09 mm
Modulus ($\hat{E}$)	28.65 kPa

V. Conclusion

In this paper, the tissue inclusion estimation method is proposed to quantify absolute stiffness and geometric parameters of tissue inclusion. The estimation is performed based on the tactile data obtained by the tactile sensation imaging system. The experimental results showed that the proposed estimation method estimates size, depth, and Young's modulus of tissue inclusions with root mean squared errors of 1.25 mm, 2.09 mm, and 28.65 kPa, respectively. This work is the initial step toward achieving for early malignant tumor detection and characterization using the tactile sensation imaging system and associated parameter estimation method.

References

[1] T. A. Krouskop, T. M. Wheeler, F. Kallel, B. S. Garra, and T. Hall, "Elastic moduli of breast and prostate tissues under compression," *Ultrason. Imaging*, vol. 20, no. 4, pp. 260–274, 1998.

[2] L. Gao, K. J. Parker, R. Lerner, and S. Levinson, "Imaging of elastic properties of tissue - A review," *Ultrasound Med Biol.*, vol. 22, no. 8, pp. 959–977, 1996.

[3] B. Garra, E. Cespedes, J. Ophir, S. spratt, R. Zuurbier, C. Magnant, and M. Pennanen, "Elastography of breast lesions: Initial clinical results," *Radiol.*, vol. 202, no. 1, pp. 79–86, 1997.

[4] J. Ophir, I. Cespedes, H. Pennekanti, Y. Yazdi, and X. Li, "Elastography, a quantitative method for imaging the elasticity of biological tissues," *Ultrason. Imaging*, vol. 13, no. 2, pp. 111-134, 1991.

[5] A. Stravros, D. Thickman, M. Dennis, S. Parker, and G. Sisney, "Solid breast nodules: Use of sonography to distinguish between benign and malignant lesions," *Radiol.*, vol. 196, no. 1, pp. 79–86, 1995.

[6] K. S. Bhatia, D. D. Rasalkar, Y. P. Lee, K. T. Wong, A. D. King, Y. H. Yuen, A. T. Ahuja, "Real-time qualitative ultrasound elastography of miscellaneous non-nodal neck masses: applications and limitations," *Ultrasound Med. Biol.,* vol. 36, no. 10, pp. 1644–1652, 2010.

[7] V. Egorov and A. P. Savazyan, "Mechanical imaging of the breast," *IEEE Trans. Medical Imag.,* vol, 27, no. 9, pp. 1275–1287, 2008.

[8] H. Yegingil, W. Y. Shih, and W.-H Shih, "All-electrical palpation shear modulus and elastic modulus measurement using a piezoelectric cantilever with a tip," *J. Appl. Phys.*, 101, 054510, 2007.

[9] P. S. Wellman, E. P. Dalton, D. Krag, K. A. Kern, and R. D. Howe, "Tactile imaging of breast masses: First clinical report," *Arch. Surg.*, vol. 136, no. 2, pp. 204–208, 2001.

[10] G. Weber, G., Using Tactile Images to Differentiate Breast Cancer Types. Division of Engineering and Applied Sciences. Cambridge, Harvard University, 2000.

[11] J. Dargahi, S. Najarian, R. Ramezanifard, and F. T. Ghomshe, "Fabrication and testing of a medical surgical instrument capable of detecting simulated embedded lumps," *Am. J. Appl. Sci.,* vol. 4, no. 12, pp. 957–964, 2009.

[12] J.-H. Lee and C.-H. Won, "High resolution tactile imaging sensor using total internal reflection and non-rigid pattern matching algorithm," *IEEE Sensors J.*, DOI: 10.1109/JSEN.2011.2109038, IEEE Early Access Version, 2011.

[13] G. S. Rajan, G. S. Sur, J. E. Mark, D. W. Schaefer, and G. Beaucage, "Preparation and characterization of some unusually transparent poly (dimethylsiloxane) nanocomposites," *J. Polymer. Sci. B Polymer Phys.*, vol. 41, pp. 1987–1901, 2003.

[14] B. E. Saleh and M. C. Teich, *Fundamentals of photonics*, Wiley-Interscience, 1991.

[15] C. M. Bishop, "Pattern Recognition and Machine Learning," *Information science and statistics*, Springer, 2007.

[16] R. Picard and D. Cook, "Cross-validation of regression models". *J. Amer. Statistical Assoc.*, vol. 79 no. 387, pp. 575–583, 1984.